Optimization Studies of the FERMI at ELETTRA FEL Design

G. De Ninno*, Sincrotrone Trieste, Trieste, Italy,
W.M. Fawley, G.E. Penn, LBNL, Berkeley, CA 94720, USA
W.S. Graves, MIT-Bates Laboratory, Middleton MA 01949 USA

Abstract

The FERMI at ELETTRA project at Sincotrone Trieste involves two FEL's, each based upon the principle of seeded harmonic generation and using the existing ELETTRA injection linac at 1.2 GeV beam energy. Scheduled to be completed in 2008, FEL-1 will operate in 40 – 100 nm wavelength range and will involve one stage of harmonic up-conversion. The second undulator line, FEL-2, will begin operation two years later in the 10 – 40 nm wavelength range and use two harmonic stages operating as a cascade. The FEL design assumes continuous wavelength tunability over the full wavelength range, and polarization tunability of the output radiation including vertical or horizontal linear as well as helical polarization. The design considers focusing properties and segmentation of realizable undulators and available input seed lasers. We review the studies that have led to our current design. We present results of simulations using *GENESIS* and *GINGER* simulation codes including studies of various shot-to-shot fluctuations and undulator errors. Findings for the expected output radiation in terms of the power, transverse and longitudinal coherence are reported.

INTRODUCTION

FERMI@Elettra[1] will be a new source of extremely bright photon beams in the UV to soft x-ray regime constructed next to the existing third generation synchrotron light source ELETTRA. FERMI will employ the present ELETTRA linac (partially upgraded for FEL operation) and a completely new photo-injector of the SLAC/BNL/UCLA-type [2], resulting in a high quality electron beam with energy $\approx 1.2\,\mathrm{GeV}$, charge $\sim 0.3 - 1.0\,\mathrm{nC}$, current $\sim 400 - 800\,\mathrm{A}$, slice emittance $\varepsilon_N \leq 1.5$ mm-mrad, and slice rms energy spread ≈ 200 keV. Two separate undulator chains will individually cover the output wavelength ranges of 100 to 40 nm (FEL-1) and 40 to 10 nm (FEL-2), respectively, providing radiation that is continuously tuneable in wavelength and polarization. The FEL's are based on the principle of seeded harmonic generation[3] with the longitudinal coherence properties of the radiation output following that of the input seed laser.

Our present design relies upon a Low-Gain-Harmonic-Generation (LGHG) approach, whose layout is shown in Fig. 1 [4]. First, a coherent input signal from a conventional UV laser ($240\,\mathrm{nm} \leq \lambda_0 \leq 300\,\mathrm{nm}$) enters an undulator (the "modulator") simultaneously with the electron beam and resonantly modulates the energy of a short slice of the electron bunch. To accomplish this, the laser seed is much shorter than the electron bunch. Immediately downstream, a chromatic dispersive section converts the energy modulation into strong spatial microbunching, with each microbunch having a large harmonic content. The electron beam then enters a second undulator (the "radiator") whose strength is set to induce resonant, coherent emission at a harmonic of the seed wavelength λ_0/n with n typically in the range 3-6. FEL-1 is a single stage device (see Fig. 1), while FEL-2 is a two stage device whose second stage modulator uses radiation from the first stage radiator. The final radiators of each FEL will be of APPLE type for full polarization control, while the modulators will be linearly polarized.

In the LGHG approach, the combination of high input seed power and dispersive sections produces sufficient micro-bunching to permit relatively short undulator lengths (*i.e.*, $L_u \leq 2\,L_{gain}$) which radiate with essentially coherent spontaneous emission. In the case of FEL-2, a temporal delay chicane is placed following the radiator of the first stage. This is used to shift the FEL light onto an unused part of the electron bunch in the "fresh-bunch" seeding approach[5], so that the electrons' instantaneous energy spread has not been increased by upstream FEL interaction. We are also examining an alternative "whole bunch" approach in which the entire electron beam is modulated and radiates in successive undulators. This alternative does not require a delay chicane or second modulator but likely requires somewhat longer total undulator lengths to reach the same output power levels.

We first discuss how various limitations and self-consistent accelerator simulations [2, 6] have led to our current LGHG design. We then present results of numerical, time-steady simulations with the *GENESIS* and *GINGER* codes including the output sensitivity to various shot-to-shot input parameter fluctuations and the effects of transverse offset and tilt errors.

DESIGN CONSIDERATIONS

To achieve maximum stability we have elected to keep the electron energy fixed while achieving wavelength tunability by varying the rms undulator strength a_u. This choice simplifies the linac design but introduces complexity into the undulator design. To determine the optimum undulator parameters, we have set the minimum a_u to be unity at the shortest wavelength of each FEL to obtain reasonable performance, and the minimum pole-to-pole gap to

* giovanni.deninno@elettra.trieste.it

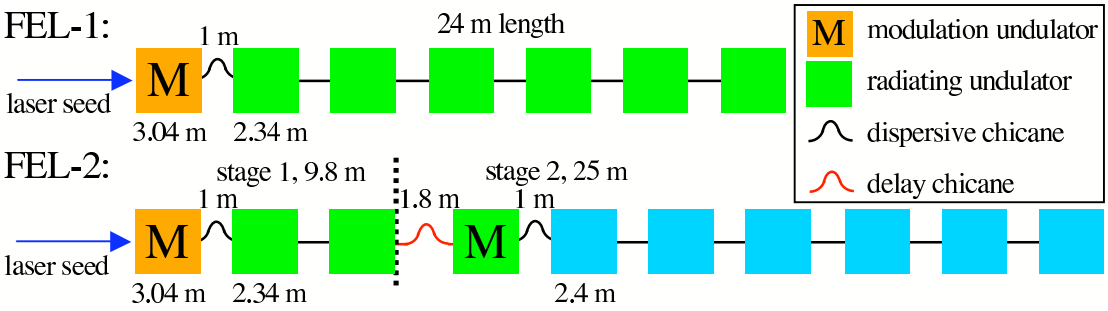

Figure 1: Layout of undulator beamlines for FEL-1 and FEL-2.

be 11 mm, which determines the maximum field strength achievable for APPLE undulators in vertical polarization. This determines the maximum a_u and longest resonant wavelength possible. With these constraints, we have settled upon undulator periods of 65 mm for the FEL-1 radiator and for both the first-stage radiator and second stage modulators of FEL-2. For the FEL-2 second stage radiator, we have chosen a period of 50 mm.

Due to both mechanical strength and diagnostic access considerations, each radiator will be segmented. The breaks between segments will be $\sim$ 1 m in length to accomodate beam diagnostics, a focusing quadrupole, dipole corrector magnets, and a longitudinal phase corrector. The only exception occurs between the two stages of FEL-2, where a 1.82-m break length permits more extensive diagnostics and the temporal delay chicane necessary for the fresh bunch approach.

An alternating-gradient quadrupole lattice with a singlet in each break between undulator sections provides the dominant electron beam focusing. Preliminary studies have shown that an average beta function of approximately 10 m yields good FEL performance. Smaller beta functions can slightly improve the output power but at the expense of mode quality, especially in FEL-1; below 6 m the increasing angular spread within the electron beam degrades the performance. In order to avoid extreme variations in the beta function (keeping the maximum and minimum beta function within a factor of 2) as well as to accomodate different configurations without encountering resonances, we have chosen a typical distance of 3.4 m between quadrupoles and thus 2.4 m of active length per undulator segment. The quadrupoles are assumed to be 0.20 m in length which corresponds to typical gradients of 5 T/m or less. The quadrupole strengths must be adjustable in order to compensate for changes in the (relatively weak) undulator focusing as the polarization and/or resonant wavelengths are changed.

The FEL-1 and FEL-2 first stage modulators are a special case because they need only to be resonant with the laser input seed and thus cover a relatively narrow resonant wavelength range (nominally 240 – 300 nm). An existing 160-mm period, linearly-polarized undulator having 3.04 m of active length may be available to the FERMI project and we have adopted these parameters for our simulation studies. For the nominal input laser seed power of 100 MW, the resulting energy modulation of roughly 1.4 MeV is well suited for downstream harmonic generation. The FEL-1 and first stage FEL-2 radiator segments will have 36 active periods (2.34-m segment length) and 1.04-m break lengths. Although the FEL-1 radiator must be capable of variable polarization, the first stage FEL-2 radiator is likely to have fixed linear polarization. For the second stage FEL-2 radiator, we have adopted 48-active-period sections (2.4-m segment length) separated by 1.0-m breaks.

FEL-1 OUTPUT PERFORMANCE

Studies of FEL-1 were undertaken with particular emphasis on output radiation at 100, 60, and 40 nm from seed wavelengths of 300, 240, and 240 nm respectively. These studies were performed with linearly polarized undulators. We adopted electron beam parameters of 1.2 GeV, 800 A, $\varepsilon_N = 1.5$ mm-mrad, and rms $\sigma_E = 200$ keV. The evolution of power and bunching with distance as calculated by *GINGER* and *GENESIS* are shown in Figs. 2 and 3. Undulators with horizontal polarization have been assumed throughout. Agreement between the two codes is good, especially at small z, although there is a noticeable discrepancy at larger z for the 60-nm case. Saturation occurs earliest in z at the longest wavelengths. At 100 nm, the output power barely grows after three 2.34-m undulator sections. At 60 nm, the output power reaches a maximum after four sections, and at 40 nm the maximum occurs after five sections. In the studies below, each wavelength case is simulated only through enough radiator segments to reach saturation, as if the gap in any downstream undulator segment was completely open. For example, the 100-nm case uses three active undulator sections.

One of the key considerations in the sensitivity studies is the dependence of output power upon jitter in the electron beam energy. In Fig. 4, the power normalized to its peak value is shown as a function of the electron energy offset. The shortest wavelengths exhibit the narrowest acceptance in energy; at 40 nm, a relative energy deviation of 2.5×10^{-3} is sufficient to reduce the output power by half.

The effect of misalignment of the electron beam has also been considered. In Fig. 5, the variation of output power

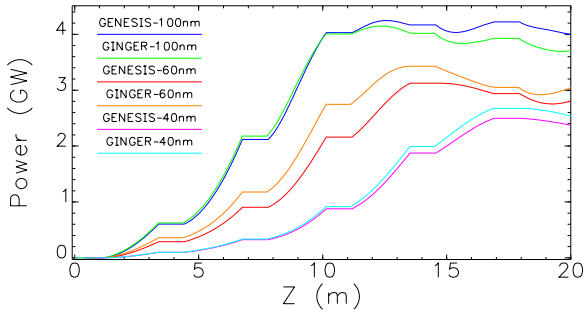

Figure 2: Plot of power vs. z for FEL-1 at 100, 60, and 40-nm wavelengths. Comparison of *GINGER* and *GENESIS* simulation results.

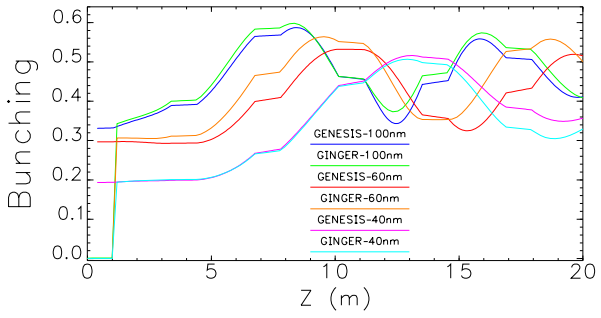

Figure 3: Plot of bunching vs. z for FEL-1 at 100, 60, and 40-nm wavelengths. Comparison of *GINGER* and *GENESIS* simulation results.

due to an initial offset or tilt in the electron beam at the first undulator is shown. The tilt is normalized to units of length by multiplying by 10 m, which is the average beta function. This yields the typical displacement which results from a given tilt. It is clear that the FEL is much more sensitive to an initial offset in the modulating undulator than to an initial tilt. Reducing the physical overlap of the electron beam with the laser seed is the most important effect of electron beam offsets. In Fig. 6, the variation in mode quality as measured by the M^2 parameter, is shown for the same electron beam offsets. Here, $M^2 \equiv 2\pi r_0 \theta_{\rm rms}/lambda$, where $lambda$ is the radiation wavelength, $\theta_{\rm rms}$ is the rms angle of the radiation, and r_0 is the rms radius of the apparent waist of the radiation. The mode quality analysis subtracts out any misalignments of the output radiation field, which are comparable to the misalignments of the electron beam. Shorter wavelengths are more sensitive to offsets because of the small divergence angles of the output radiation.

In Table 1, the sensitivity of output power and phase to relative variations in energy, current, energy spread, and emittance are shown. The values from *GENESIS* simulations at nominal parameters are given, as well as first and second derivates with respect to each parameter.

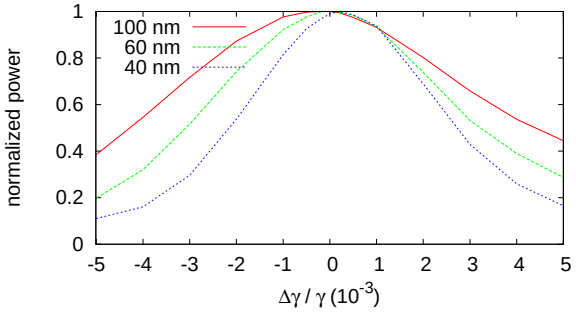

Figure 4: Plot of power reduction due to variation in electron beam energy for FEL-1 at 100, 60, and 40-nm wavelengths. Data are from *GENESIS* simulations.

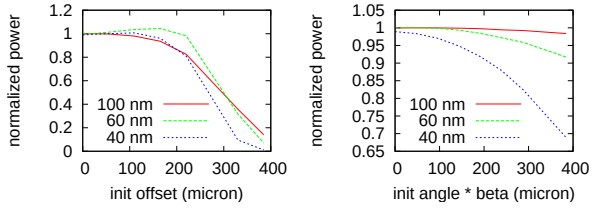

Figure 5: Plot of power reduction due to initial displacement (left) and tilt (right), for FEL-1 at 100, 60, and 40-nm wavelengths. Tilts are normalized to the beta function. Data are from *GENESIS* simulations.

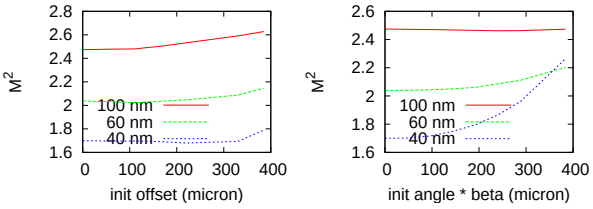

Figure 6: Plot of M^2 as a function of initial displacement (left) and tilt (right), for FEL-1 at 100, 60, and 40-nm wavelengths. Tilts are normalized to the beta function. Data are from *GENESIS* simulations.

FEL-2 OUTPUT PERFORMANCE

Studies of FEL-2 were undertaken at wavelengths of 40, 20, and 10 nm. The first stage of FEL-2 is much like FEL-1, except only two radiating undulator segments are used, and they do not need to be APPLE-type undulators. Before the second stage, the beam passes through a temporal delay chicane, followed by a single modulating undulator before entering the final set of radiating undulators. The 40-nm final radiation was seeded by 80-nm light from the first stage using a 240-nm laser seed, and the 20 and 10-nm outputs used 40-nm light from the first stage also starting from a 240-nm laser seed. The electron beam parameters are the same as in FEL-1. The evolution of power and bunching with distance as calculated by *GINGER* and *GENESIS* are shown in Figs. 7 and 8. There is good agreement between

Table 1: Sensitivity of output power and phase to electron beam jitter for FEL-1 at 100, 60, and 40-nm wavelengths. Results from nominal parameters are given, as well as scaled first and second derivatives with respect to electron beam parameters.

	100 nm		60 nm		40 nm	
$f =$	P (GW)	Φ (rad)	P (GW)	Φ (rad)	P (GW)	Φ (rad)
f	4.03	-2.04	3.12	1.01	2.50	2.69
$\gamma\, df/d\gamma$	-92.4	-3840	24.4	-5440	150	-7210
$\gamma^2\, d^2f/d\gamma^2$	-4.5×10^5	-1.1×10^5	-5.0×10^5	-0.7×10^5	-6.7×10^5	-1.1×10^5
$I\, df/dI$	7.35	2.37	5.08	2.34	4.07	2.39
$I^2\, d^2f/dI^2$	-0.68	-1.00	-3.20	0.99	-3.48	-1.32
$\sigma_\gamma\, df/d\sigma_\gamma$	-1.14	-0.51	-0.61	-0.92	-0.40	-1.20
$\sigma_\gamma^2\, d^2f/d\sigma_\gamma^2$	-1.04	-0.20	-1.92	0.62	-2.04	-3.00
$\epsilon\, df/d\epsilon$	-2.08	-0.83	-1.18	-0.80	-0.97	-0.86
$\epsilon^2\, d^2f/d\epsilon^2$	2.44	5.80	-3.76	5.54	-6.68	5.12

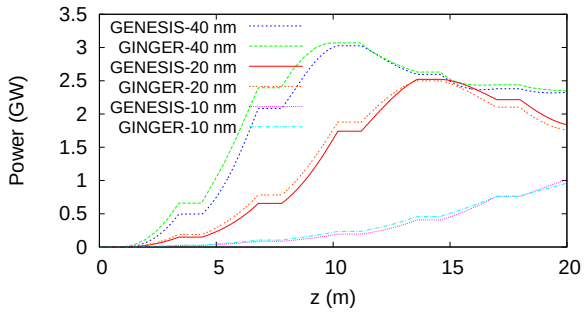

Figure 7: Plot of power vs. z for FEL-2 at 40, 20, and 10-nm wavelengths. Comparison of *GINGER* and *GENESIS* simulation results.

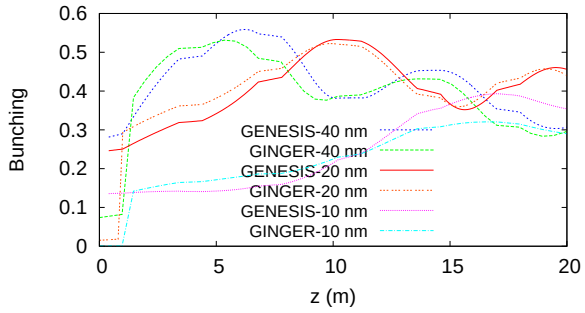

Figure 8: Plot of bunching vs. z for FEL-2 at 40, 20, and 10-nm wavelengths. Comparison of *GINGER* and *GENESIS* simulation results.

the two codes. As in FEL-1, saturation occurs earliest in z at the longest wavelengths. At 40 nm, the output power saturates after three sections, at 20 nm, the output power reaches a maximum after four sections, and at 10 nm all six sections add to the output radiation power. In the studies below, each wavelength case is simulated only until saturation is reached.

In Figure 9, the power normalized to its peak value is shown as a function of the electron energy offset. As in

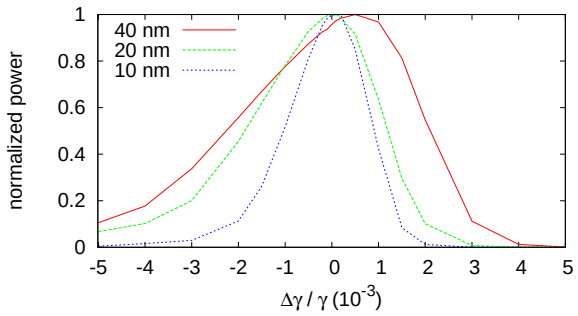

Figure 9: Plot of power reduction due to variation in electron beam energy for FEL-2 at 40, 20, and 10-nm wavelengths. Data are from *GENESIS* simulations.

FEL-1, the acceptance in electron beam energy continues to decrease as the wavelength is decreased; at 10 nm, a relative energy deviation of 1×10^{-3} is sufficient to reduce the output power by half. In fact, the energy acceptance for the 40-nm cases in both FEL-1 and FEL-2 are nearly identical. This suggests that there is no additional sensitivity to electron energy introduced by going through multiple stages; however, the 10-nm case does exhibit a strong sensitivity to energy jitter and chirp coming from the linac.

REFERENCES

[1] C. Bocchetta *et al.*, in these proceedings.

[2] S. Lidia *et al.*, in these proceedings.

[3] L.H. Yu *et al.*, Phys. Rev. Lett. 91, 74801 (2003).

[4] G. Penn *et al.*, "Harmonic Cascade FEL Designs for LUX", Proceedings of EPAC 2004, 488, Lucerne, CH (2004). Available at http://www.JACoW.org/.

[5] I. Ben-Zvi, K. M. Yang, and L. H. Yu, *Nucl. Inst. Meth. A*, **318**, 726 (1992).

[6] S. Di Mitri *et al.*, in these proceedings.